Supplementary Information

Elucidating O_2 Reduction Reaction on 2D Monolayer $LaMnO_3$ Perovskite

Naveen Sharma[1] and Srimanta Pakhira[1, 2*]

[1] *Theoretical Condensed Matter Physics & Advanced Computational Materials Science Laboratory*, Department of Physics, Indian Institute of Technology Indore, Khandwa Road, Simrol, Indore,453552, MP, India.

[2] *Theoretical Condensed Matter Physics & Advanced Computational Materials Science Laboratory*, Centre for Advanced Electronics (CAE), Indian Institute of Technology Indore, Khandwa Road, Simrol, Indore, 453552, MP, India.

*Corresponding author: spakhira@iiti.ac.in (or) spakhirafsu@gmail.com

S1: AIMD Stability Analysis of the 3D $LaMnO_3$ and 2D LMO perovskites at 500 K

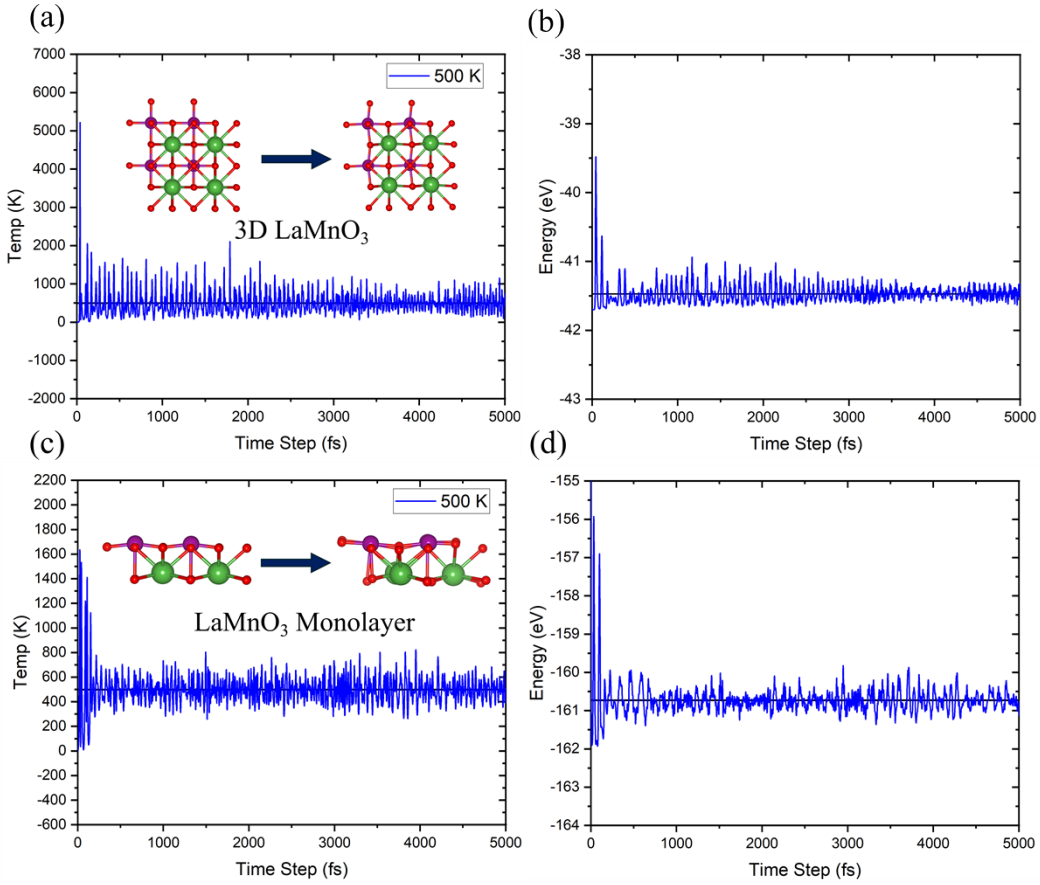

Fig. S1 Ab initio molecular dynamics (AIMD) simulations at 500 K for bulk and two-dimensional $LaMnO_3$. (a) Temperature evolution and (b) total energy fluctuations of 3D $LaMnO_3$ as a function of time steps, demonstrating thermal equilibration and energy stability. (c) Temperature evolution and (d) total energy fluctuations of 2D $LaMnO_3$ monolayer under the same conditions. Insets show the corresponding structural configurations before and after AIMD, confirming the thermal stability of both bulk and monolayer $LaMnO_3$ at elevated temperature.

S2: ORR Steps and Free Energy Analysis

Step I. To obtain the equilibrium structure of the 2D LMO with O_2 adsorbed at the Mn-active site, the PBE-D method was utilized as stated earlier. Fig. 5a (see main text) shows equilibrium structure of the 2 x 2 supercell of the 2D LMO. The equilibrium structure and bond lengths of the reaction intermediate [O_2_$LaMnO_3$] is shown in Fig. 5b, and the calculated values of bond lengths of Mn–O, and O–O are 1.89 Å and 1.28 Å respectively (reported in Table 3). The equilibrium structure of [O_2_$LaMnO_3$] has P1 symmetry with the equilibrium lattice constants a = 7.38 Å, b = 7.40 Å and $\alpha = 89.75°, \beta = 91.48°$ – obtained by the same PBE-D method used in

the present investigation (See Table 3 in the main text). Fig. S2a shows the electronic band structure and TDOS for both spin up and down states of the [O_2_$LaMnO_3$], above and below the E_F. To compute the band structure, GGA+U method has been employed and a high symmetric path $\Gamma - X - M - \Gamma$ has been chosen in the first Brillouin zone. From Fig. S3a it could be concluded that this reaction intermediate has a wide band gap with presence of large number of electronic density of states in spin-up channel for conduction, pertaining to the half-metallic nature of the intermediate.

Step II. During the next step, the protonation of [O_2_$LaMnO_3$] takes place leading to the formation of [OOH_$LaMnO_3$] intermediate in the reaction and its equilibrium geometry is shown in Fig. 5c (See main text). The equilibrium lattice constants of this intermediate are calculated to be a = 7.38, b = 7.41 Å, α = 89.29°, β = 91.31° and it has P1 symmetry. The equilibrium bond lengths for Mn–O, O–O and O–H have been calculated to be 1.84 Å, 1.46 Å, and 0.98 Å, respectively (See Table 3 in the main text). This intermediate also shows a conducting nature which can be concluded from Fig. S3b which shows an overlap of bands, and significant electronic density at the E_F. The highly symmetric k-path $\Gamma - X - M - \Gamma$ is used for band structure calculations. In this intermediate step the free energy change ΔG for the formation is calculated to be -0.22 eV and a relative free energy change from the previous step is -0.61 eV (See Table 2 in the main text).

Step III. Next the computational PBE-D calculation is performed for [O_$LaMnO_3$] intermediate (See Fig. 5d in the main text) and resulted equilibrium lattice constants are a = b = 7.33 Å and angles, α = 89.90°, β = 91.91° (See Table 3 in the main text). Here the calculated bond length of Mn–O is found to be 1.57 Å. During this step the water molecule is released leading to a free energy change of -0.78 eV and a relative free energy change of -1.40 eV. The band structure plot and total density of states are shown in Fig. S3c, overlapping of bands and the presence of significant electron density at the E_F confirms that this intermediate is conducting in nature.

Step IV. The last intermediate which forms during the associative mechanism before removal of second water molecule and resulting in the original 2D monolayer LMO perovskite is [OH_$LaMnO_3$] (shown in Fig. 5e). The calculated equilibrium lattice constants are a = 7.39 Å, b = 7.41 Å, and α = 89.84°, β = 92.86° using the PBE-D method (See Table 3 in the main text). The structure shows P1 symmetry. The equilibrium bond lengths of Mn–O, and O–H are found to be

1.82 Å and 0.97, respectively. The free energy change in this step is calculated to be -2.41 eV (Table 2) and the relative free energy change is calculated as -3.82 eV (See Table 2 in the main text). The electronic band structure is calculated along the high symmetric path $\Gamma - X - M - \Gamma$ and is shown in Fig. S3d.

Step V. In the dissociative mechanism there are two additional steps after step I of the associative mechanism, which involves dissociation of the adsorbed O_2 on surface of the 2D LMO perovskite. This dissociation leads to the formation of intermediate [2O_$LaMnO_3$] (See Fig. 7c in the main text). Here the oxygen atom from the oxygen molecule adsorbed on the Mn site has migrated to another Mn active site on the surface of the monolayer. The equilibrium lattice constants of the complex are a = 7.31 Å, b = 7.24 Å, and α = 89.85º, β = 89.74º with P1 symmetry. The new Mn–O bond formed at both the Mn active sites of [2O_$LaMnO_3$] is an unstable bond with a positive value of free energy change of 2.41 eV (See Table 5 in the main text). The calculated bond length of Mn–O is about 1.58 Å. The equilibrium lattice constants 'a' and 'b' have decreased slightly by an amount of 0.07 Å, and 0.16 Å, respectively. For the electronic property calculations of intermediate [2O_$LaMnO_3$], a highly symmetric $\Gamma - X - M - \Gamma$ k-path is chosen. The plots obtained for band structure and TDOS are shown in Fig. S3e. The intermediate shows good conductivity with overlap of bands and high density of states at the E_F.

Step VI. The equilibrium 2D monolayer structure of the [OH_O_$LaMnO_3$] intermediate during the dissociative mechanism of the ORR is shown in Fig. 7d (See main text). The lattice constants of this intermediate are a = 7.36 Å, b = 7.41 Å and $\alpha = \beta$ = 89.79º with P1 symmetry. The bond lengths of Mn–O, and O–H is calculated to be 1.78 Å, 1.65 Å, and 0.95 Å. The electronic band structures and total DOS for the intermediate are shown in Fig. S3f. The equilibrium parameters and bond lengths of all the intermediates of the dissociative mechanism are listed in Table 4.

S3: Electronic band structure and total density of states plots for all intermediates occurring during associative and dissociative mechanism on surface of the 2D LMO perovskite.

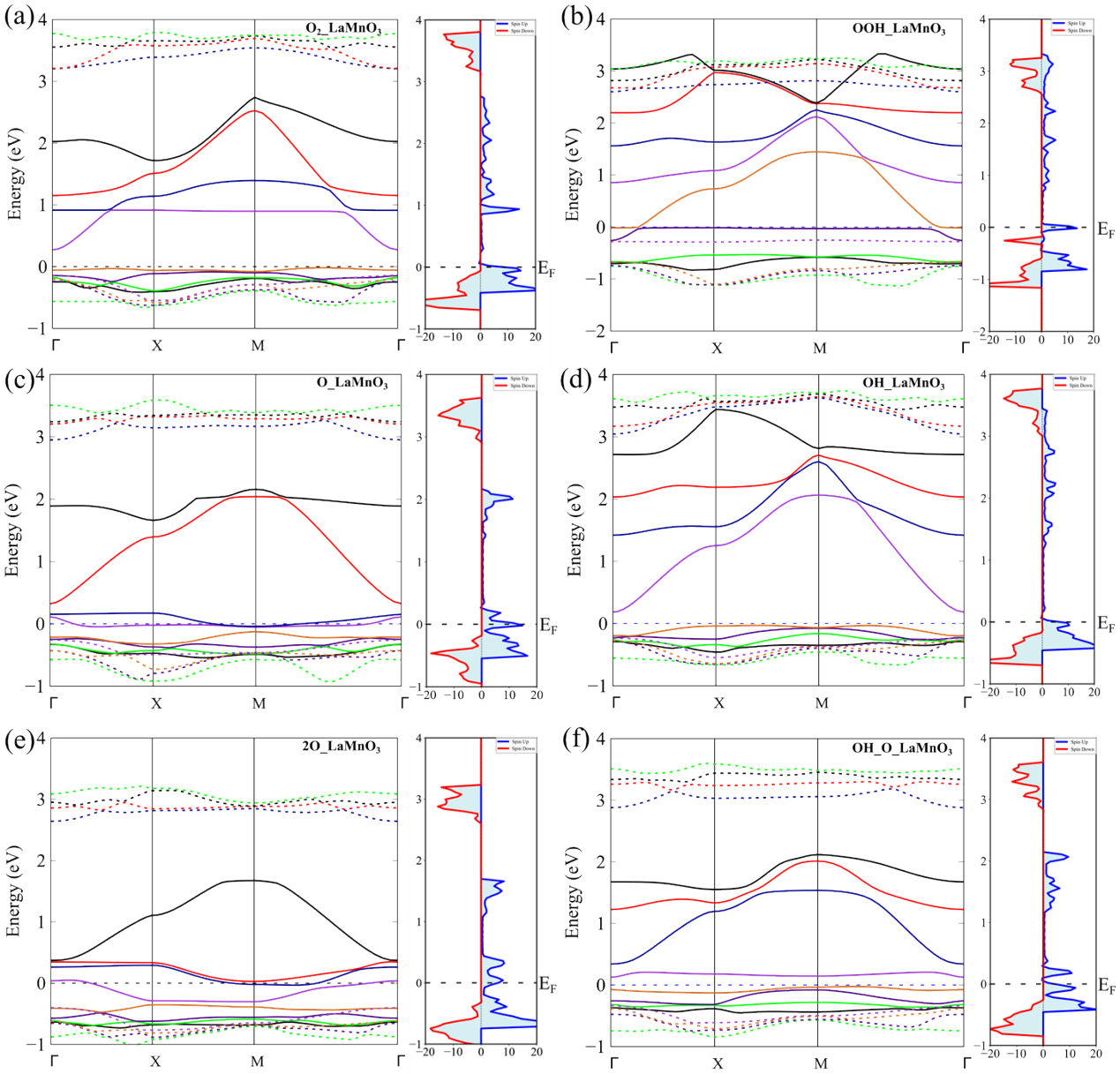

Fig. S3 Electronic structure properties i.e., electronic band structure and TDOS plots for (a) [O_2_$LaMnO_3$] (b) [OOH_$LaMnO_3$] (c) [O_$LaMnO_3$] (d) [OH_$LaMnO_3$] (e) [2O_$LaMnO_3$] (f) [OH_O_$LaMnO_3$] reaction intermediates involved in both associative and dissociative mechanism. (In band structure plots the dotted and solid lines represent spin-down and spin-up states, respectively, and, in TDOS plots the blue and red lines represent total spin-up and spin-down densities respectively).

S4: Optimized structures of 3D $LaMnO_3$ cubic perovskite, 2D LMO and various intermediates occurring during associative and dissociative mechanism of ORR (.cif format)

1. Optimized structures (.cif format) for 3D $LaMnO_3$ perovskite and 2D LMO.

1.1. Optimized structures (.cif format) for 3D $LaMnO_3$ perovskite.

```
_cell_length_a                         3.895149
_cell_length_b                         3.895114
_cell_length_c                         3.895213
_cell_angle_alpha                      90.001411
_cell_angle_beta                       89.999504
_cell_angle_gamma                      90.002037
_cell_volume                           59.098361
_space_group_name_H-M_alt              'P 1'
_space_group_IT_number                 1

loop_
_space_group_symop_operation_xyz
  'x, y, z'

loop_
  _atom_site_label
  _atom_site_occupancy
  _atom_site_fract_x
  _atom_site_fract_y
  _atom_site_fract_z
  _atom_site_adp_type
  _atom_site_U_iso_or_equiv
  _atom_site_type_symbol
  La1      1.0    0.000233    0.000010    0.000096
  Mn1      1.0    0.500465    0.500012    0.500103
  O1       1.0   -0.000037    0.500104    0.499750
  O2       1.0    0.499864    0.499791    0.000444
  O3       1.0    0.499475    0.000084    0.499607
```

1.2. Optimized structures (.cif format) for 2D LMO.

```
_cell_length_a                         7.411957
_cell_length_b                         7.411950
_cell_length_c                         14.425076
_cell_angle_alpha                      89.998177
_cell_angle_beta                       90.000908
_cell_angle_gamma                      89.999870
_cell_volume                           792.471153
```

```
_space_group_name_H-M_alt                'P 1'
_space_group_IT_number                   1

loop_
_space_group_symop_operation_xyz
  'x, y, z'

loop_
  _atom_site_label
  _atom_site_occupancy
  _atom_site_fract_x
  _atom_site_fract_y
  _atom_site_fract_z
  _atom_site_adp_type
  _atom_site_U_iso_or_equiv
  _atom_site_type_symbol
  La1     1.0   0.496744   0.498044   0.419073
  La2     1.0   0.996744   0.498041   0.419075
  La3     1.0   0.496743   0.998042   0.419074
  La4     1.0   0.996743   0.998044   0.419073
  Mn1     1.0   0.246754   0.248065   0.287700
  Mn2     1.0   0.746754   0.248065   0.287701
  Mn3     1.0   0.246754   0.748065   0.287701
  Mn4     1.0   0.746755   0.748065   0.287700
  O1      1.0   0.246756   0.498063   0.303458
  O2      1.0   0.496754   0.248065   0.303459
  O3      1.0   0.246786   0.248079   0.450116
  O4      1.0   0.746761   0.498066   0.303458
  O5      1.0   0.996757   0.248064   0.303460
  O6      1.0   0.746789   0.248079   0.450119
  O7      1.0   0.246759   0.998067   0.303458
  O8      1.0   0.496758   0.748064   0.303458
  O9      1.0   0.246793   0.748079   0.450120
  O10     1.0   0.746757   0.998062   0.303458
  O11     1.0   0.996754   0.748065   0.303461
  O12     1.0   0.746787   0.748077   0.450116
```

2. Optimized structures (.cif format) for ORR intermediates

2.1. For O_2_$LaMnO_3$

```
_cell_length_a                           7.380970
_cell_length_b                           7.401631
_cell_length_c                           14.589537
```

```
_cell_angle_alpha                       89.751373
_cell_angle_beta                        91.486572
_cell_angle_gamma                       90.005554
_cell_volume                            796.768360
_space_group_name_H-M_alt               'P 1'
_space_group_IT_number                  1

loop_
_space_group_symop_operation_xyz
  'x, y, z'

loop_
  _atom_site_label
  _atom_site_occupancy
  _atom_site_fract_x
  _atom_site_fract_y
  _atom_site_fract_z
  _atom_site_adp_type
  _atom_site_U_iso_or_equiv
  _atom_site_type_symbol
  La1     1.0   0.496806   0.503819   0.422152
  La2     1.0   1.001292   0.493552   0.419217
  La3     1.0   0.497474   0.991366   0.422039
  La4     1.0   1.000686   1.001524   0.419077
  Mn1     1.0   0.244098   0.248722   0.285910
  Mn2     1.0   0.737950   0.248853   0.290205
  Mn3     1.0   0.241605   0.748752   0.286899
  Mn4     1.0   0.741524   0.748666   0.289721
  O1      1.0   0.244435   0.498235   0.304236
  O2      1.0   0.492588   0.248729   0.317807
  O3      1.0   0.233832   0.247999   0.452484
  O4      1.0   0.741028   0.498898   0.309707
  O5      1.0   0.991853   0.248653   0.299023
  O6      1.0   0.763065   0.246727   0.444015
  O7      1.0   0.692977   0.252405   0.161991
  O8      1.0   0.530482   0.249057   0.127715
  O9      1.0   0.244644   0.998942   0.304426
  O10     1.0   0.492268   0.748351   0.304305
  O11     1.0   0.256884   0.746907   0.450905
  O12     1.0   0.740622   0.998430   0.308698
  O13     1.0   0.992643   0.748620   0.305637
  O14     1.0   0.741314   0.748623   0.452040
```

2.2. For 2O_$LaMnO_3$

_cell_length_a	7.311123
_cell_length_b	7.248048
_cell_length_c	14.939903
_cell_angle_alpha	89.850952
_cell_angle_beta	89.749802
_cell_angle_gamma	89.999916
_cell_volume	791.675743
_space_group_name_H-M_alt	'P 1'
_space_group_IT_number	1

loop_
_space_group_symop_operation_xyz
'x, y, z'

loop_
_atom_site_label
_atom_site_occupancy
_atom_site_fract_x
_atom_site_fract_y
_atom_site_fract_z
_atom_site_adp_type
_atom_site_U_iso_or_equiv
_atom_site_type_symbol

La1	1.0	0.497517	0.491983	0.424244
La2	1.0	0.996392	0.488186	0.422867
La3	1.0	0.497493	1.004032	0.424193
La4	1.0	0.996393	1.007773	0.422810
Mn1	1.0	0.250924	0.248880	0.270302
Mn2	1.0	0.745375	0.248879	0.270424
Mn3	1.0	0.247840	0.748664	0.296546
Mn4	1.0	0.747766	0.748680	0.294484
O1	1.0	0.248623	0.489320	0.310524
O2	1.0	0.497953	0.248660	0.310684
O3	1.0	0.240291	0.247704	0.459589
O4	1.0	0.746915	0.489734	0.310010
O5	1.0	0.997537	0.248653	0.303217
O6	1.0	0.750910	0.247749	0.459311
O7	1.0	0.731336	0.249730	0.163895
O8	1.0	0.248672	1.007889	0.310359
O9	1.0	0.497764	0.748529	0.309608
O10	1.0	0.248835	0.747941	0.446476
O11	1.0	0.746860	1.007490	0.309860

O12	1.0	0.997579	0.748575	0.309905
O13	1.0	0.743155	0.747916	0.448041
O14	1.0	0.266901	0.249734	0.164521

2.3. For OH_O_$LaMnO_3$

_cell_length_a	7.364667
_cell_length_b	7.410289
_cell_length_c	14.936282
_cell_angle_alpha	89.787331
_cell_angle_beta	89.797447
_cell_angle_gamma	90.017479
_cell_volume	815.126580
_space_group_name_H-M_alt	'P 1'
_space_group_IT_number	1

loop_
_space_group_symop_operation_xyz
'x, y, z'

loop_
_atom_site_label
_atom_site_occupancy
_atom_site_fract_x
_atom_site_fract_y
_atom_site_fract_z
_atom_site_adp_type
_atom_site_U_iso_or_equiv
_atom_site_type_symbol

La1	1.0	0.495311	0.501426	0.419812
La2	1.0	0.996634	0.493150	0.415944
La3	1.0	0.495408	0.994172	0.419560
La4	1.0	0.996831	1.002615	0.415781
Mn1	1.0	0.252886	0.249070	0.284338
Mn2	1.0	0.740643	0.248931	0.287883
Mn3	1.0	0.246627	0.748752	0.293720
Mn4	1.0	0.746616	0.748748	0.293897
O1	1.0	0.247387	0.496036	0.309390
O2	1.0	0.496572	0.248604	0.324193
O3	1.0	0.240412	0.247658	0.443941
O4	1.0	0.745933	0.498080	0.309688
O5	1.0	1.001217	0.248514	0.303840
O6	1.0	0.755908	0.247761	0.441346

O7	1.0	0.685331	0.251149	0.171400
O8	1.0	0.247646	1.001301	0.308825
O9	1.0	0.496395	0.748132	0.305818
O10	1.0	0.247520	0.747936	0.444197
O11	1.0	0.746273	0.999090	0.309484
O12	1.0	0.997084	0.748309	0.304993
O13	1.0	0.745469	0.747890	0.444600
O14	1.0	0.317380	0.252418	0.177937
H1	1.0	0.556837	0.269187	0.161482

2.4. For O_$LaMnO_3$

_cell_length_a	7.331739
_cell_length_b	7.333526
_cell_length_c	15.052051
_cell_angle_alpha	89.900948
_cell_angle_beta	91.918373
_cell_angle_gamma	90.000740
_cell_volume	808.856263
_space_group_name_H-M_alt	'P 1'
_space_group_IT_number	1

loop_
_space_group_symop_operation_xyz
'x, y, z'

loop_
_atom_site_label
_atom_site_occupancy
_atom_site_fract_x
_atom_site_fract_y
_atom_site_fract_z
_atom_site_adp_type
_atom_site_U_iso_or_equiv
_atom_site_type_symbol

La1	1.0	0.500098	0.497666	0.419777
La2	1.0	0.994513	0.492928	0.418751
La3	1.0	0.500294	0.998284	0.419722
La4	1.0	0.994311	1.003061	0.418697
Mn1	1.0	0.239541	0.248399	0.293717
Mn2	1.0	0.735021	0.248626	0.273273
Mn3	1.0	0.239105	0.748405	0.296018
Mn4	1.0	0.738963	0.748405	0.293390

O1	1.0	0.241050	0.497056	0.302851
O2	1.0	0.496762	0.248387	0.313399
O3	1.0	0.244240	0.247949	0.445806
O4	1.0	0.739105	0.491801	0.309884
O5	1.0	0.982887	0.248449	0.306220
O6	1.0	0.759089	0.247505	0.457002
O7	1.0	0.714369	0.249637	0.168716
O8	1.0	0.241027	0.999683	0.302790
O9	1.0	0.492249	0.748335	0.303163
O10	1.0	0.253990	0.747722	0.447523
O11	1.0	0.739083	1.004980	0.309552
O12	1.0	0.989587	0.748325	0.302104
O13	1.0	0.748278	0.748149	0.445916

2.5. For OH_$LaMnO_3$

_cell_length_a	7.399041
_cell_length_b	7.412848
_cell_length_c	14.578036
_cell_angle_alpha	89.849152
_cell_angle_beta	92.865540
_cell_angle_gamma	90.018456
_cell_volume	798.573095
_space_group_name_H-M_alt	'P 1'
_space_group_IT_number	1

loop_
_space_group_symop_operation_xyz
'x, y, z'

loop_
_atom_site_label
_atom_site_occupancy
_atom_site_fract_x
_atom_site_fract_y
_atom_site_fract_z
_atom_site_adp_type
_atom_site_U_iso_or_equiv
_atom_site_type_symbol

La1	1.0	0.498133	0.502587	0.419480
La2	1.0	1.000528	0.497818	0.418987
La3	1.0	0.498688	0.993588	0.419307
La4	1.0	1.000217	0.997975	0.419008

Mn1	1.0	0.235149	0.248579	0.292159
Mn2	1.0	0.736078	0.248738	0.291325
Mn3	1.0	0.235693	0.748700	0.287731
Mn4	1.0	0.736680	0.748711	0.290340
O1	1.0	0.238265	0.499283	0.305921
O2	1.0	0.487117	0.249133	0.306398
O3	1.0	0.243434	0.248327	0.450502
O4	1.0	0.737781	0.499901	0.308263
O5	1.0	0.986809	0.248230	0.300271
O6	1.0	0.756320	0.247442	0.440193
O7	1.0	0.711090	0.251466	0.166338
O8	1.0	0.238682	0.997833	0.306244
O9	1.0	0.487268	0.748396	0.304287
O10	1.0	0.256577	0.747486	0.451402
O11	1.0	0.737796	0.997343	0.307644
O12	1.0	0.988517	0.748584	0.306833
O13	1.0	0.746907	0.748536	0.452822
H1	1.0	0.581121	0.267327	0.153018

2.6. For OOH_$LaMnO_3$

_cell_length_a	7.387187
_cell_length_b	7.418750
_cell_length_c	14.657871
_cell_angle_alpha	89.294807
_cell_angle_beta	91.316254
_cell_angle_gamma	90.017738
_cell_volume	803.032722
_space_group_name_H-M_alt	'P 1'
_space_group_IT_number	1

loop_
_space_group_symop_operation_xyz
'x, y, z'

loop_
_atom_site_label
_atom_site_occupancy
_atom_site_fract_x
_atom_site_fract_y
_atom_site_fract_z
_atom_site_adp_type
_atom_site_U_iso_or_equiv

_atom_site_type_symbol

La1	1.0	0.495058	0.502926	0.420294
La2	1.0	1.000074	0.495174	0.418746
La3	1.0	0.496380	0.990433	0.420079
La4	1.0	0.998928	0.997817	0.418487
Mn1	1.0	0.241562	0.249747	0.290757
Mn2	1.0	0.739874	0.249673	0.294195
Mn3	1.0	0.240570	0.749853	0.288048
Mn4	1.0	0.741028	0.749664	0.291634
O1	1.0	0.242898	0.499974	0.306600
O2	1.0	0.491727	0.249569	0.312838
O3	1.0	0.232916	0.247106	0.451437
O4	1.0	0.740718	0.501218	0.310433
O5	1.0	0.991155	0.249672	0.297047
O6	1.0	0.758645	0.244646	0.438838
O7	1.0	0.731915	0.258291	0.168496
O8	1.0	0.546628	0.261257	0.129964
O9	1.0	0.243071	0.998809	0.306745
O10	1.0	0.490851	0.749143	0.305664
O11	1.0	0.253492	0.745313	0.451677
O12	1.0	0.740266	0.997943	0.307680
O13	1.0	0.992326	0.749300	0.307306
O14	1.0	0.740533	0.748897	0.453251
H1	1.0	0.574454	0.219884	0.068434